Learning from Outside the Viability Kernel:
Why we Should Build Robots that can Fall With Grace

Steve Heim and Alexander Spröwitz

Abstract— Despite impressive results using reinforcement learning to solve complex problems from scratch, in robotics this has still been largely limited to model-based learning with very informative reward functions. One of the major challenges is that the reward landscape often has large patches with no gradient, making it difficult to sample gradients effectively. We show here that the robot state-initialization can have a more important effect on the reward landscape than is generally expected. In particular, we show the counter-intuitive benefit of including initializations that are *unviable*, in other words initializing in states that are doomed to fail.

I. INTRODUCTION

Recent advances in reinforcement learning (RL) have shown a lot of promise, especially with the capability to learn complex policies from scratch, model-free and from very generic reward signals [1][2]. However it has been difficult to transfer these results into learning directly in robot hardware. Most RL in robotics is model-based and uses highly informative reward functions [3].

One of the main challenges is that much of the reward landscape (sometimes called a cost landscape) that a learning algorithm needs to traverse tends to be flat, providing no informative gradient. In classical RL, the ability to run a huge number of trials, often in parallel, with completely random initial conditions for both state and policy parameters helps alleviate the problem. With a robot, this can be prohibitively expensive in terms of time, hardware costs and computation. It is typically necessary to invest substantial effort into the design of a reasonable initial controller and parameterization, and subsequently improve it via RL [4][5], instead of learning policies from scratch.

Another common approach is to rely on model-based control methods, and use RL to learn the model, instead of learning the policy [3][6].

It is also important to choose an appropriate exploration strategy, and the subfield of intrinsic motivation in particular addresses the problem of getting stuck in a flat portion of the reward landscape [7]. Alternatively, the reward landscape can be shaped by providing more informative reward functions [8][9], or a progressive set of reward functions or environments [10][11][12][13].

While these approaches all have merit, we show that the choice of state initialization can have a greater effect on the reward landscape than is usually assumed. The current practice is to initialize from a stable state, as states that fail

Dynamic Locomotion Group, Max Planck Institute for Intelligent Systems, Stuttgart, DE {heim, sprowitz}@.is.mpg.de

with a high probability can be crippling. Quick failures often result in no reward and therefore no gradient to learn from, and often damage the robot hardware itself. At the most restrictive, this means the robot always starts within the basin of attraction of a stable controller. In order to accelerate learning, it is important for the learning agent to explore outside this region, and indeed considerable effort has been made to be able to step outside the basin of attraction and into its superset [14][15], the *viability kernel*.

A viability kernel [16] is the set of all states from which there is at least one time-evolution that remains confined to a desired region. Sampling states outside the current policy's basin of attraction allows the agent to learn more aggressively and still avoid potentially disastrous failures. When learning a model of the dynamics, the agent can clearly benefit by being even more aggressive and initially visit failure states. These states will often be in areas of the state-space that are otherwise not visited, and data-points sampled there can give additional information to fit a model more accurately. When directly learning a policy in a model-free approach however, the benefit of visiting states from which no stabilizing policy exists is less obvious.

The main contribution of this work is to show that it can be beneficial for model-free learning to initialize the robot from states *outside the viability kernel*.

II. VIABILITY KERNEL OF A RUNNING MODEL

A. Model

Our work revolves around the spring-loaded inverted pendulum (SLIP) model, a hybrid dynamic model ubiquitous in both biomechanics and the robotic legged-locomotion community for modeling running or hopping gaits. This model can be fit very accurately to experimental data of many different running animals [17][18], allows accurate prediction [19], and also has been used to design controllers for simulations [20][21][22][23] as well as actual robots [24][25][26]. Indeed, there has been a lot of effort to give legged robots SLIP-like behavior, either through mechanical design [27][28] or control [24][29]. The two dimensional view of the model, in the sagittal plane parallel to the direction of travel, represents a submanifold of the 3D-space, and the results can be extended to 3D motion both in simulation [23] and hardware [30].

We consider this an ideal model that is both low-dimensional enough to clearly illustrate our result, while also informative and applicable to real-world systems. The model, shown in Fig. 1, has a point mass representing the body center of gravity, and a massless spring representing
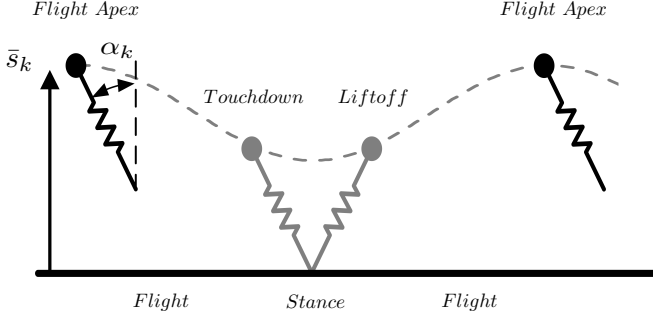
Fig. 1: The classical spring-loaded inverted pendulum is characterized by hybrid dynamics: the governing equations of motion switch between flight and stance phases at the touchdown and liftoff events. We have highlighted here the normalized height at apex $\bar{s}_k$ as our one-dimensional state and the landing angle of attack α_k as our one-dimensional action.

the leg. Touchdown and liftoff conditions govern the switch between flight and stance phases. The model uses a no-slip assumption for the foot during stance phase. At liftoff, the massless leg is instantaneously reset to the landing angle of attack α_k. The continuous dynamics are as follow:

Continuous Dynamics

Flight Dynamics

$$\begin{bmatrix} \ddot{x} \\ \ddot{y} \end{bmatrix} = \begin{bmatrix} 0 \\ -g \end{bmatrix}$$

Stance Dynamics

$$\begin{bmatrix} \ddot{x} \\ \ddot{y} \end{bmatrix} = \frac{k}{m}(l_0 - l) \begin{bmatrix} \sin(\alpha) \\ \cos(\alpha) \end{bmatrix} - \begin{bmatrix} 0 \\ g \end{bmatrix}$$

Touchdown Condition

$$y = l_0 \cos(\alpha_k)$$

Liftoff Condition

$$l = l_0$$

$$\alpha = \arctan(y/x) - \frac{\pi}{2}$$
$$l = \sqrt{((x - x_f)^2 + y^2)}$$

x : horizontal position l_0 : leg resting length = 1 [m]

y : vertical position k : spring stiffness = 8200 [N/m]

α : angle of attack α_k : landing angle of attack [rad]

x_f : foot position m : body mass = 80 [kg]

l : leg length g : gravity constant = 9.81 [m/s^2]

The parameters used are parameters commonly used to model human running [31].

As is commonly done [20][21][32], we use Poincaré return maps to study the system [33]. We numerically integrate the continuous-time dynamics from one apex height to the next, and examine the state at these apex events. This gives us the following discrete mapping:

Discrete Dynamics
Continuous Dynamics Integrated from Apex to Apex

State at Apex

$$s_k = \begin{bmatrix} y_{apex} \\ \dot{x}_{apex} \end{bmatrix}$$

Normalized Height at Apex

$$\bar{s}_k = \frac{E_g}{E_g + E_k} = \frac{g\, y_{apex}}{\frac{\dot{x}_{apex}^2}{2} + gy_{apex}}$$

Apex Transition Dynamics
$$\bar{s}_{k+1} = P(\bar{s}_k, \alpha_k)$$

E_g : Potential Energy
E_k : Kinetic Energy
P : Poincaré map

We drop the x coordinate as it is not periodic, and at apex the $\dot{y}$ coordinate is zero by definition, which leaves us with only two coordinates, y and $\dot{x}$. Finally, we exploit the fact that the system is energy-conservative and use the constant total energy constraint to reduce the system to a single state, a normalized hopping height. This results in the map $\bar{s}_{k+1} = P(s_k, \alpha_k)$. Note that we include the landing angle of attack parameter α_k as a control input which can be chosen freely at each apex. The original passive model was used to analyze steady-state locomotion and set α_k as a constant parameter; for non-steady-state locomotion, the landing angle of attack is a well studied choice for a control input [23][30][34], alongside spring-stiffness.

B. Transition Matrix and Viability Kernel

The discrete dynamics of the system have two possible transitions: either a mapping from one apex height to the next apex height, or from an apex height to a failure state, in which the point-mass body hits the ground with $\bar{s}_{k+1} = 0$.

Having reduced both state and action space to a single dimension, we obtain the entire transition matrix by brute force simulation of a finely discretized grid over $\bar{s}$ and α_k, use this to compute a difference in state and visualize the result in Fig. 2. The grey regions are failures ending with the body hitting the ground, and the colored regions are all the state-action combinations that result in a second hop. The warm colored region represent actions that lead to a higher height at the next apex, whereas the cold-colored region are actions that result in a lower height at the next apex. The intersection between these two regions are limit-cycles where the apex height remains constant. As the end-goal of locomotion is
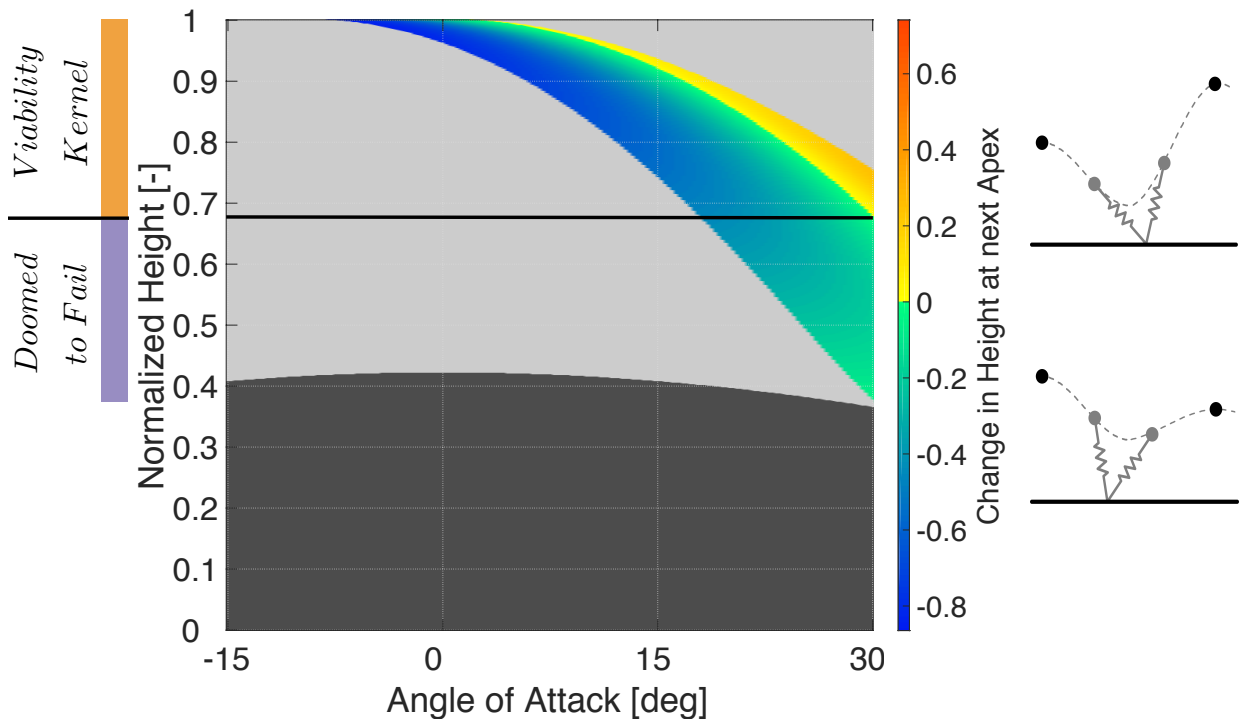
Fig. 2: Represented is the change in state for the SLIP model, with an energy content of $E_g + E_k = 1.86 kJ$. The grey regions represent state-action pairs that result in falls, and the black regions are infeasible points: the foot would start underground at apex. The warm colored region result in a higher apex height, whereas the cold colored region results in a lower apex height. The black line at normalized height 0.675 indicates the lower bound of the viability kernel: any states below this height can only select actions that lead to a lower hopping height, until it inevitably falls.

arguably to reach a specific distance, actually traveling on a limit-cycle is not strictly necessary: a policy which hops erratically can also reach the end-goal. The black region represents state-action combinations that are infeasible: the foot would start underground at apex.

This constraint between 0° and 30° for α_k is convenient to illustrate our case, while also corresponding to the usual range of angles used in human running [31]. It is also a realistic constraint a robot might need to cope with, for example due to mechanical hard-stops, limitations in hip-swing velocity or to remain within friction cones.

The viability kernel of this constrained SLIP-model can be seen by inspecting Fig. 2, and is the set of normalized apex heights $\bar{s}_k \in [0.675, \ 1]$. For each state in this set, actions can be chosen that either keep the system on a limit-cycle, bring it to a higher, or to a lower apex height. Thus, it is always possible to stay inside the set, making it a viability kernel [16]. Any state that starts below the normalized height threshold of 0.675, marked with a horizontal line in Fig. 2, can only choose actions that either immediately fall or at best hop at subsequently lower apex heights until it falls. These states are *doomed to fail*.

III. CONTROL AND LEARNING

In our study, our goal is to learn a control policy for choosing α_k at each apex which travels as far as possible from any viable initial state without falling.

A. Control Policy

Various control policies have been proposed for SLIP models, often emphasizing deadbeat control [23][34] or some form of optimality [20][35]. At its simplest, even a linear controller is able to stabilize any of the limit cycles, even if not in an optimal manner. We limit this study to a linear controller, visualized in Fig. 3, since its low dimensionality allows us to directly visualize the reward landscape in parameter space, as in Fig. 4. The core of our results depends on the structure of the transition matrix (the dynamics) both inside and outside the viability kernel, which is independent of the parameterization used.

Specifically, we use a linear gaussian policy

$$\alpha_k \sim \mathcal{N}(\mu, \sigma^2)$$
$$\mu = \theta_0 s_k + \theta_1$$

where $\mathcal{N}$ is the normal distribution, μ is the mean and represents the greedy policy in absence of exploration, and σ^2 is the variance (our exploration parameter). The parameters θ_0 and θ_1 are the slope and offset of our linear policy[1]. Gaussian policies effectively include exploration directly into the policy and are often effective in continuous state and action systems, as often encountered in robotics [2][3].

---

[1]Though technically affine, we use the common practice of calling this linear to avoid confusion.
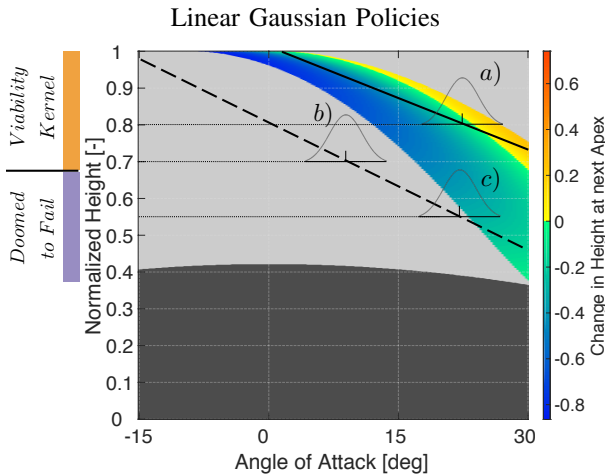
Fig. 3: Represented are two linear controllers. The solid line is a well-tuned controller that would effectively stabilize the system, whereas dashed line is a guess that has the correct general shape, but is far from the salient gradient set (SGS). To highlight the problem, we have overlaid the gaussian sampling for three possible situations: in *a)* the gaussian policy would sample with high probability from the SGS for a state inside the viability kernel. With the second greedy controller in *b)* however, the probability of sampling a non-failing action is close to 0. Case *c)* shows that the second greedy controller has a decent chance of sampling successfully from the SGS when initialized outside the viability kernel. It can learn from these samplings even though all initializations are doomed to fail.

B. Interplay of Parameter Initialization, State Initialization and Exploration Strategy

As an illustrative example, we award a fixed reward at each apex, which equates to learning to hop as many times as possible, regardless of the initial conditions. Using other periodic rewards, such as distance traveled per step, does not change the quality of the results.

It is clear that in order to learn, the agent needs to sample at least once a state-action pair that transitions to another apex: if the agent immediately samples from the state-action pairs that result directly in a fall, colored grey in Fig. 2, it will have a constant reward of 0 and no gradient to learn from. For convenience, we will call the set of state-action pairs that result in a second apex height a *salient gradient set (SGS)*.

With a random initialization of the policy parameters θ_0 and θ_1, it is possible that the greedy policy lies completely outside the SGS of the transition matrix, and therefore has a low chance of sampling from the SGS. The standard solution of increasing the variance of the gaussian policy has a drawback. While it increases the probability of sampling from the SGS when the greedy policy is initialized far away from the SGS, it also increases the probability to sample failing actions when the greedy policy is well tuned, as visualized with the solid line in Fig. 3.

In this work, we highlight another aspect of the problem which, to the best of our knowledge, has been largely overlooked. In fig. 3 we show an example where the greedy policy chooses an action far from the salient gradient set for

any state belonging to the viability kernel. In these cases, even local exploration will have only a low probability of ever taking a second step and receiving a reward. The same policy has a high probability of sampling non-failing actions for states *outside* the viability kernel. In other words, we can directly change the reward landscape by including these states in the state initialization.

C. Landscapes

We discretized over the parameters θ_0 and θ_1, computed 100 roll-outs for each point of the grid using a fixed exploration rate σ and used the average return as an estimate of the reward. We then interpolated over the grid to obtain the reward landscapes.

We repeated this for two scenarios: strictly *viable initializaiton* (left column in Fig. 4) and *feasible initializations* (right column in Fig. 4. Viable initializations are initial states sampled with a uniform distribution from the viability kernel, whereas feasible initializations are sampled from a uniform distribution of all feasible states, including states that are doomed to fail.

We have also repeated this estimate for different variance, to highlight the much greater effect the state initialization has on the reward landscape. Indeed we found that using feasible initialization increased the SGS by just over 79%. Nearly doubling the variance, from 8° to 15°, only increased the SGS by 13%. This highlights a case where a large effort to find effective exploration strategies can be replaced with an improved state initialization.

D. Learning Setup and Results

To test our results, we implemented a standard temporal-difference algorithm with eligibility trace, a typical policy-gradient class of reinforcement learning algorithms [2][36] relying on the likelihood ratio [37] to estimate the policy gradient. To find appropriate hyperparameters for the learning step size and discount factor, several hundred learning trials were run with randomized hyperparameters, which revealed most consistent performance with a very low discount factor around 0.95, and learning step sizes on the order of magnitude of 0.001; in the presented results, these values are used. The variance of the gaussian policy begins at 15° and is reduced to 10°, 7.5° and 5° as the average performance reaches 2, 3 and 4 steps respectively. Once a policy averages at least 15 steps, learning is terminated.

To compare learning performance we ran learning trials starting from the same initial policy parameter, using first only viable initializations and then feasible initializations. In the second case, once the policy averages more than three steps, we consider the policy to have learned sufficiently and switch to a viable initialization, since the end-goal is to be stable for viable initializations.

We first ran trials for 50 randomized policy initializations (see Fig. 5). Before accepting each randomly selected policy initialization, its performance is estimated by averaging the reward over 100 roll-outs with viable initialization, as we did when estimating the reward landscape. Policy parameters

Reward Landscapes

Landscapes with Viable Initialization

Landscapes with Feasible Initialization
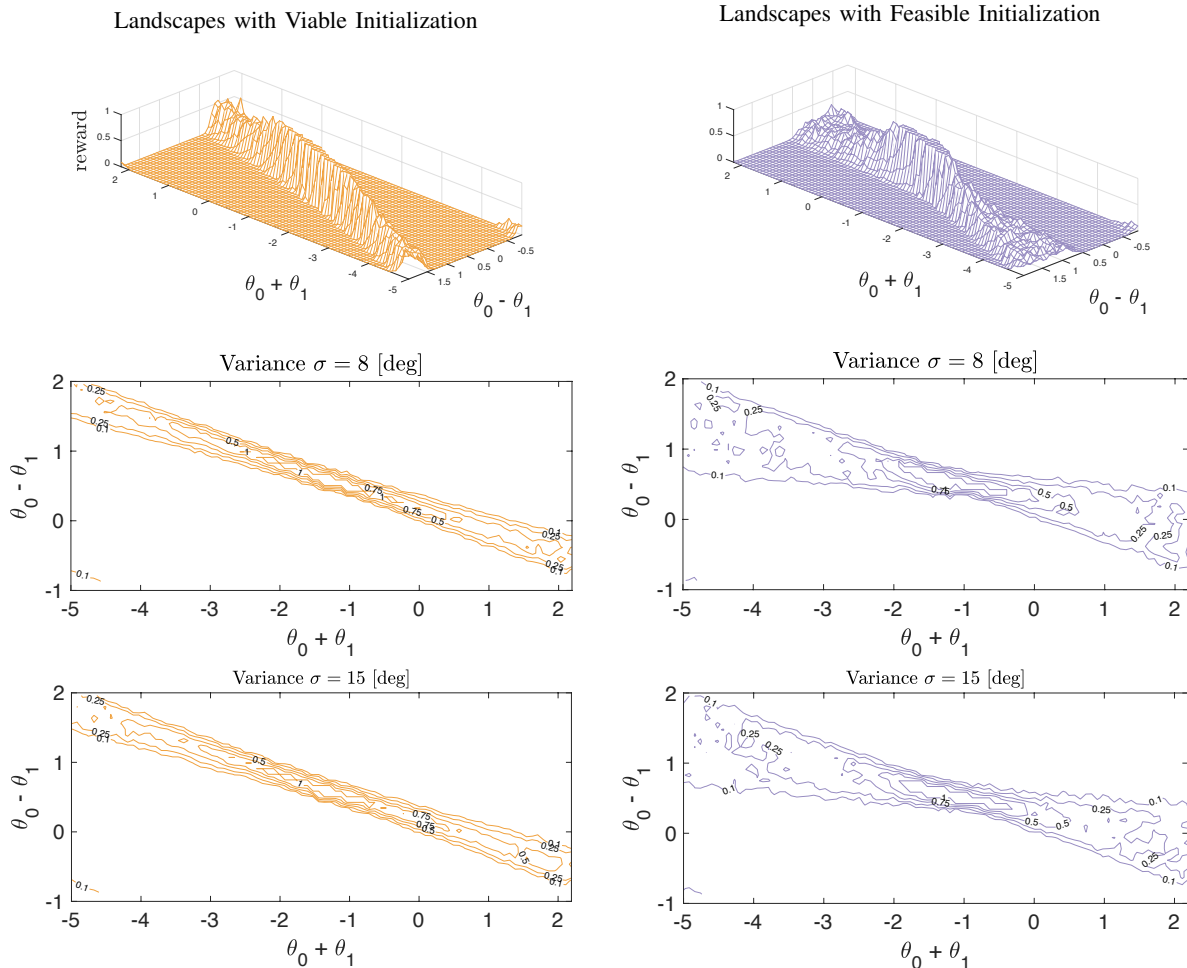
Fig. 4: In the reward landscapes on the left, the system is initialized with a uniform random sampling inside the viability kernel, whereas on the right it is initialized from states with a feasible action, whether viable or doomed to fail. For visual clarity, the parameter space has been rotated 45 degrees and the reward (number of steps taken) is capped at 1. At values greater than this, the gradient is very steep and policies quickly become stable for many steps. The meshed landscapes (top row) are shown for clarity and are the same as the first set of contours (second row) with variance of 8°. The landscape on the right has a salient gradient set (a point in parameter space with non-zero gradient) just over 79% larger. The landscapes with a more aggressive variance of 15° (bottom row) are shown to highlight how little effect increasing exploration has in comparison to the choice in state initialization.

with less than 0.5 steps on average are discarded and re-sampled. In other words, we biased initializations towards policy parameters for which viable initializations also had a chance to learn, instead of including policy parameters where viable initializations had no chance of learning.

As shown in Fig. 5, we found that starting with feasible initializations resulted in 60% more trials ending in success. The policy initializations relative to the landscapes is shown in Fig. 6. We then selected a single parameter at random, and repeated 10 trials each with viable and feasible initializations, shown in Fig. 7. Again, we found much greater reliability in learning success when starting from feasible initialization rather than strictly viable initializations.

IV. DISCUSSION AND OUTLOOK

We show the effect state initialization has on the reward landscape of a dynamically unstable system, and a clear case where a naive policy initialization learns more reliably when unviable states, that is states that are doomed to fail, are included in the initializations. We have in particular highlighted it is to consider the effect of state initialization in overcoming a common problem in robot learning: reward landscapes with large patches devoid of gradient information. This adds another tool to design learning setups, in addition to more established approaches of exploration strategies or reward shaping.

One of the major drawbacks of initializing in unviable states is that failures often result in damage to the robot. A solution is to start learning in simulation before transferring the policies to real robots [38][39]. With this approach, it

Rate of Success for Randomized Initial Policies
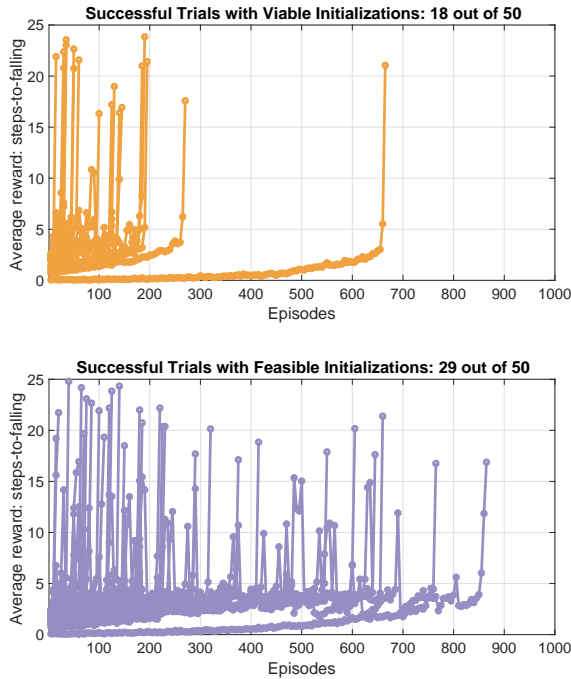
Fig. 5: Fifty initial policy parameters were tested, sampled at random with a minimum chance of taking a 0.5 steps on average when using a viable initialization. For visual clarity, only successful trials are plotted.

is important not to mirror the same conditions of the robot in simulation, but purposefully explore with more aggressive and potentially unviable initializations.

While this approach is promising, a simulation still relies on a model even if the policy is learned model-free. One of the attractions of model-free learning is the reduced need for expert knowledge and engineering effort in order to directly deploy robots in the field. To this end, our results suggest a different emphasis for robot design is needed. A robot should not only be mechanically sturdy so it can survive failures, but there should be meaningful actions to be explored in unviable states. As we show with the SLIP model (see Fig. 2), the choice to fall immediately or to stumble several steps before falling is what allows the system to learn from unviable states. This is a property of the system dynamics, and therefore the hardware design and not the controller design. Especially when building legged robots that try to mimic a SLIP-like behavior [27][28], these aspects should be considered in addition to measures such as passive stability and energy efficiency.

REFERENCES

[1] D. Silver, J. Schrittwieser, K. Simonyan, *et al.*, "Mastering the game of go without human knowledge", *Nature*, vol. 550, no. 7676, pp. 354–359, 2017.

[2] R. S. Sutton and A. G. Barto, *Reinforcement learning: An introduction*, 1. MIT press Cambridge, 1998, vol. 1.
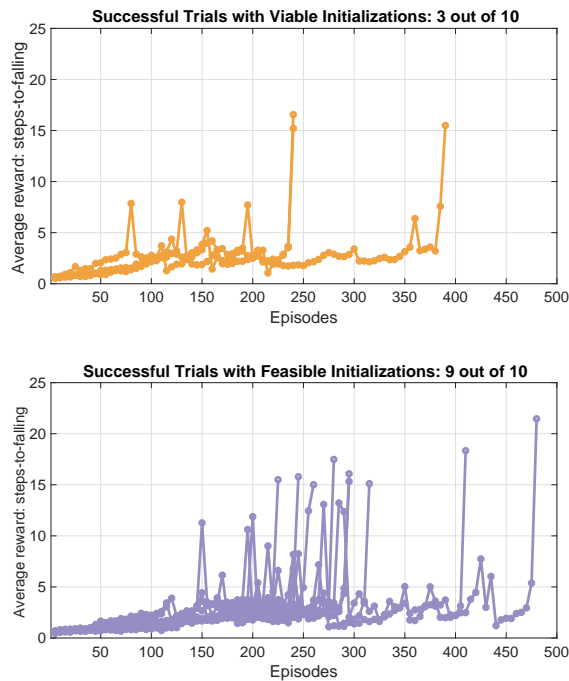
Trial Policy Parameters
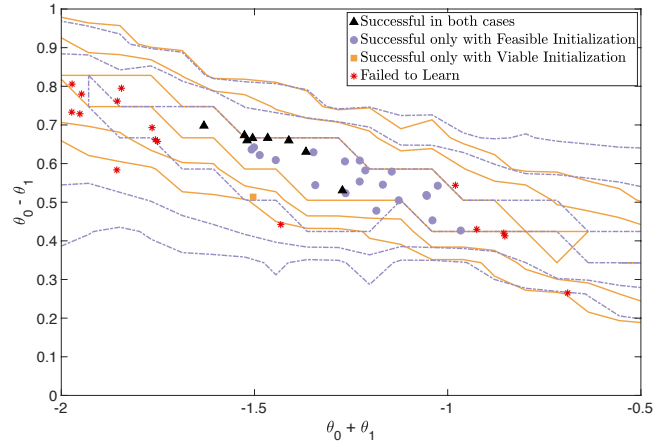
Fig. 6: Examining the location of the initial policy parameters on the reward landscape shows just how brittle the viable initializations are. The distribution of the parameters which fail for both initializations also suggests some further structure we have not explored here. The landscape contours with viable initializations (solid orange line) and feasible initializations (dashed purple line) are overlaid for reference.

[3] J. Kober, J. A. Bagnell, and J. Peters, "Reinforcement learning in robotics: A survey", *The International Journal of Robotics Research*, vol. 32, no. 11, pp. 1238–1274, 2013.

[4] E. Heijmink, A. Radulescu, B. Ponton, *et al.*, "Learning optimal gait parameters and impedance profiles for legged locomotion", in *Humanoid Robotics (Humanoids), 2017 IEEE-RAS 17th International Conference on*, IEEE, 2017, pp. 339–346.

[5] N. Kohl and P. Stone, "Policy gradient reinforcement learning for fast quadrupedal locomotion", in *Robotics and Automation, 2004. Proceedings. ICRA'04. 2004 IEEE International Conference on*, IEEE, vol. 3, 2004, pp. 2619–2624.

[6] S. Levine, N. Wagener, and P. Abbeel, "Learning contact-rich manipulation skills with guided policy search", in *Robotics and Automation (ICRA), 2015 IEEE International Conference on*, IEEE, 2015, pp. 156–163.

[7] N. Chentanez, A. G. Barto, and S. P. Singh, "Intrinsically motivated reinforcement learning", in *Advances in neural information processing systems*, 2005, pp. 1281–1288.

[8] P. Abbeel and A. Y. Ng, "Apprenticeship learning via inverse reinforcement learning", in *Proceedings of the twenty-first international conference on Machine learning*, ACM, 2004, p. 1.

[9] M. Kalakrishnan, P. Pastor, L. Righetti, *et al.*, "Learning objective functions for manipulation", in *Robotics and Automation (ICRA), 2013 IEEE International Conference on*, IEEE, 2013, pp. 1331–1336.

[10] Y. Bengio, J. Louradour, R. Collobert, *et al.*, "Curriculum learning", in *Proceedings of the 26th annual international conference on machine learning*, ACM, 2009, pp. 41–48.

[11] A. Karpathy and M. Van De Panne, "Curriculum learning for motor skills", *Advances in Artificial Intelligence*, pp. 325–330, 2012.

[12] J. Randlov and P. Alstrom, "Learning to drive a bicycle using reinforcement learning and shaping", in *Proceedings of the Fifteenth International Conference on Machine Learning*, 1998, pp. 463–471.

[13] S. Heim, F. Ruppert, A. A. Sarvestani, *et al.*, "Shaping in practice: Training wheels to learn fast hopping directly

Rate of Success for Multiple Trials

Fig. 7: Ten trials starting from the same initial policy parameters were repeated, with viable initializations (top) and feasible initializations (bottom). The improved reliability with feasible initializations is clear, with 9 out of 10 trials succeeding, compared to 3 out of 10 for the viable initializations. For visual clarity, only successful trials are plotted.

in hardware", *ArXiv preprint arXiv:1709.10273*, 2017, Accepted to Robotics and Automation (ICRA), 2018 IEEE International Conference on.

[14] S. Prajna and A. Jadbabaie, "Safety verification of hybrid systems using barrier certificates", in *International Workshop on Hybrid Systems: Computation and Control*, Springer, 2004, pp. 477–492.

[15] N. Smit-Anseeuw, R. Vasudevan, and C. D. Remy, "Safe online learning using barrier functions", *Proceedings of Dynamic Walking*, 2017.

[16] J.-P. Aubin, *Viability theory*. Springer Science & Business Media, 2009.

[17] R. Blickhan, "The spring-mass model for running and hopping", *Journal of biomechanics*, vol. 22, no. 11-12, pp. 1217–1227, 1989.

[18] R. J. Full and D. E. Koditschek, "Templates and anchors: Neuromechanical hypotheses of legged locomotion on land", *Journal of Experimental Biology*, vol. 202, no. 23, pp. 3325–3332, 1999.

[19] H.-M. Maus, S. Revzen, J. Guckenheimer, *et al.*, "Constructing predictive models of human running", *Journal of The Royal Society Interface*, vol. 12, no. 103, p. 20 140 899, 2015.

[20] T. Cnops, Z. Gan, and C. D. Remy, "The basin of attraction for running robots: Fractals, multistep trajectories, and the choice of control", in *Intelligent Robots and Systems (IROS), 2015 IEEE/RSJ International Conference on*, IEEE, 2015, pp. 1586–1591.

[21] G. Piovan and K. Byl, "Reachability-based control for the active slip model", *The International Journal of Robotics Research*, vol. 34, no. 3, pp. 270–287, 2015.

[22] İ. Uyanık, U. Saranlı, and Ö. Morgül, "Adaptive control of a spring-mass hopper", in *Robotics and Automation (ICRA), 2011 IEEE International Conference on*, IEEE, 2011, pp. 2138–2143.

[23] A. Wu and H. Geyer, "The 3-d spring–mass model reveals a time-based deadbeat control for highly robust running and steering in uncertain environments", *IEEE Transactions on Robotics*, vol. 29, no. 5, pp. 1114–1124, 2013.

[24] W. C. Martin, A. Wu, and H. Geyer, "Experimental evaluation of deadbeat running on the atrias biped", *IEEE Robotics and Automation Letters*, vol. 2, no. 2, pp. 1085–1092, 2017.

[25] S. Rezazadeh, C. Hubicki, M. Jones, *et al.*, "Spring-mass walking with atrias in 3d: Robust gait control spanning zero to 4.3 kph on a heavily underactuated bipedal robot", in *Proceedings of the ASME 2015 Dynamic Systems and Control Conference*, 2015.

[26] P. Terry, G. Piovan, and K. Byl, "Towards precise control of hoppers: Using high order partial feedback linearization to control the hopping robot frank", in *Decision and Control (CDC), 2016 IEEE 55th Conference on*, IEEE, 2016, pp. 6669–6675.

[27] C. Hubicki, J. Grimes, M. Jones, *et al.*, "Atrias: Design and validation of a tether-free 3d-capable spring-mass bipedal robot", *The International Journal of Robotics Research*, vol. 35, no. 12, pp. 1497–1521, 2016.

[28] D. Lakatos, W. Friedl, and A. Albu-Schäffer, "Eigenmodes of nonlinear dynamics: Definition, existence, and embodiment into legged robots with elastic elements", *IEEE Robotics and Automation Letters*, vol. 2, no. 2, pp. 1062–1069, 2017.

[29] M. Hutter, C. D. Remy, M. A. Höpflinger, *et al.*, "Slip running with an articulated robotic leg", in *Intelligent Robots and Systems (IROS), 2010 IEEE/RSJ International Conference on*, IEEE, 2010, pp. 4934–4939.

[30] M. H. Raibert, *Legged robots that balance*. MIT press, 1986.

[31] A. Seyfarth, H. Geyer, M. Günther, *et al.*, "A movement criterion for running", *Journal of biomechanics*, vol. 35, no. 5, pp. 649–655, 2002.

[32] J. Rummel and A. Seyfarth, "Stable running with segmented legs", *The International Journal of Robotics Research*, vol. 27, no. 8, pp. 919–934, 2008.

[33] E. R. Westervelt, J. W. Grizzle, C. Chevallereau, *et al.*, *Feedback control of dynamic bipedal robot locomotion*. CRC press, 2007, ch. 4.

[34] L. R. Palmer III and C. E. Eaton, "Periodic spring–mass running over uneven terrain through feedforward control of landing conditions", *Bioinspiration & biomimetics*, vol. 9, no. 3, p. 036 018, 2014.

[35] G. Piovan and K. Byl, "Two-element control for the active slip model", in *Robotics and Automation (ICRA), 2013 IEEE International Conference on*, IEEE, 2013, pp. 5656–5662.

[36] R. J. Williams, "Simple statistical gradient-following algorithms for connectionist reinforcement learning", *Machine learning*, vol. 8, no. 3-4, pp. 229–256, 1992.

[37] R. S. Sutton, D. A. McAllester, S. P. Singh, *et al.*, "Policy gradient methods for reinforcement learning with function approximation", in *Advances in neural information processing systems*, 2000, pp. 1057–1063.

[38] X. B. Peng, M. Andrychowicz, W. Zaremba, *et al.*, "Sim-to-real transfer of robotic control with dynamics randomization", *ArXiv preprint arXiv:1710.06537*, 2017.

[39] W. Yu, C. K. Liu, and G. Turk, "Preparing for the unknown: Learning a universal policy with online system identification", *ArXiv preprint arXiv:1702.02453*, 2017.